Digital Memory in Barrier-Grid Storage Tubes

By M. E. HINES, M. CHRUNEY, and J. A. McCARTHY

(Manuscript received July 2, 1955)

In barrier-grid storage tubes, a cathode ray beam is used to deposit electrostatic charge on a dielectric surface. The same beam is utilized to detect and remove the charge at a later time. This paper describes the mode of operation of such tubes when used for storage of binary digital information. The sources of variation in the output signal are discussed. A basis is given for determining the probability of error due to amplifier noise. The storage capacity and program of operation are determined by the requirement of error-free performance. A discussion is included of data obtained from experimental tubes capable of storing 16,000 bits of information with reading or writing times of about one microsecond. A new type of target-reading circuit which is particularly suited to binary storage is also described.

I. INTRODUCTION

Storage of information in barrier-grid tubes is accomplished by depositing an electrostatic charge pattern on a dielectric sheet with a cathode-ray beam and detecting the charge pattern at a later time with the same beam. This type of tube obtains its name from a fine grid placed immediately in front of the dielectric sheet. The "barrier-grid" serves to inhibit the redistribution of secondary electrons emitted from the dielectric sheet and to shield the drift space from electrostatic disturbances which would otherwise result from the stored charge pattern and the application of writing signals. Use of this type of tube for "image" storage was described by Jensen and others.[1] This paper describes the characteristics of a barrier-grid storage tube when used as a memory device for binary digital information.[2]

[1] A. S. Jensen, J. P. Smith, M. H. Mesner, and L. E. Flory, RCA Review, **9**, pp. 112–135, March, 1948.
[2] A similar tube was described by R. B. DeLano, Jr., Convention Record of the I.R.E., Part 3, pp. 125–130, 1954.

There is a wide latitude in the manner in which the tube may be operated. On the other hand, the speed of operation, the number of usable storage sites and the likelihood of error are interdependent. As the limiting storage capacity is approached, the likelihood of error increases sharply. The sources of variations in the output signals are described in this paper and a basis is given for determining the probability of error due to amplifier noise. Our discussion is concerned mainly with results obtained from experimental models of storage tubes. They utilize electrostatic beam focusing and deflection in order to permit high speed random access to any of the storage sites on the target.

A new type of reading and writing circuit was used in these investigations which is particularly suited to binary storage. The circuit allows signal detection at the storage target while maintaining good isolation between the input writing signal and the weak output reading signal.

II. OPERATING PRINCIPLES OF BARRIER-GRID TUBES

1. *Experimental Tubes*

A schematic drawing of the tube is shown in Fig. 1 and a photograph of the tube in Fig. 2. The electron gun, focusing system, and deflection

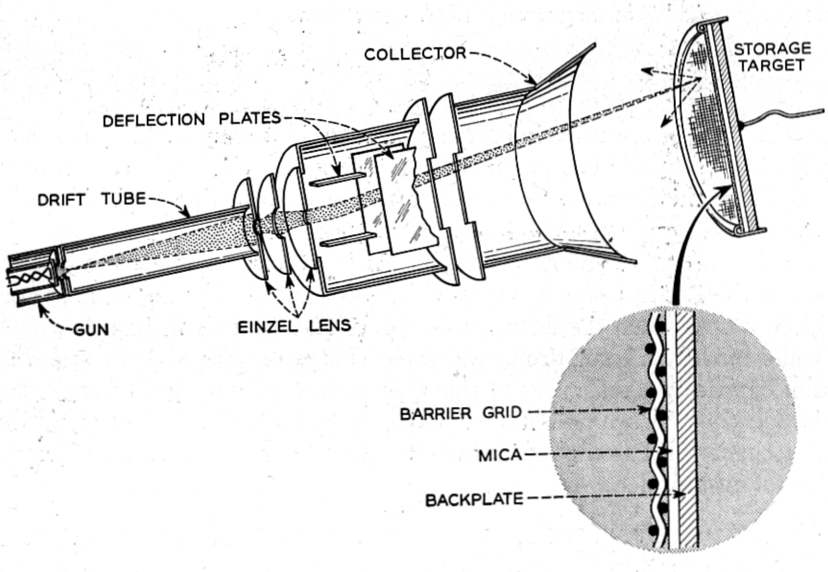

Fig. 1 — Schematic cross-section of a barrier-grid tube.

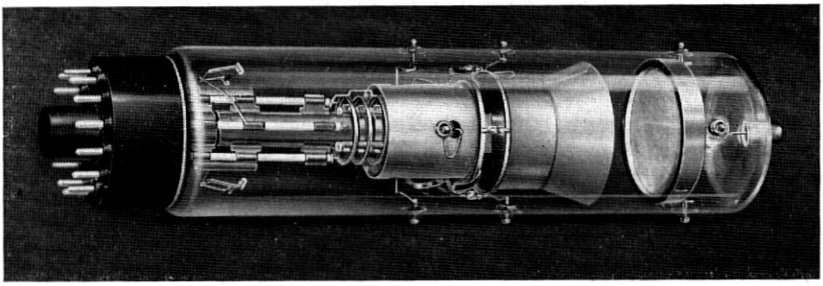

Fig. 2 — Experimental barrier-grid storage tube.

system are quite conventional and follow standard cathode-ray tube practice. The gun is a three-element immersion-lens structure of the type which produces a small crossover immediately in front of the cathode. The beam spreads outward from this crossover in an expanding cone and impinges on a limiting aperture at the end of a field-free drift tube. An Einzel type electron lens converges the trajectories of those central electrons which pass through the limiting aperture. This forms an image at the target of the first crossover in the gun. The electron beam at the target is roughly Gaussian in shape with a diameter such that the standard deviation, σ in Equation 1, of the current density distribution is about 0.002 inch. Ninety-five percent of the current will pass through a slit aperture 0.007 inch in width. The normal beam current is two microamperes and the accelerating potential is 1,000 volts.

An electron collector is placed just beyond the deflection plates to receive secondary electrons released at the storage target. The beam itself passes through a hole in the center of this collector. In one mode of operation, the signal is detected at this electrode, but in the target-reading mode, to be described later, the collector as a separate electrode is not required.

The storage target is a sandwich of three elements. A sheet of mica 0.001 inch thick is held between the barrier-grid and backplate. The grid is a woven mesh (wire cloth) of stainless steel with 400 wires per inch in each direction, the wires being 0.001 inch in diameter. These three elements are assembled to be in contact over the entire surface. The mica sheet, being a good insulator, will hold an electrostatic charge deposited on its surface for extended periods of time, thereby performing the storage function of the tube. The backplate is insulated from the grid and its potential may be varied to control the charge pattern laid down by the electron beam.

2. *Deposition of the Charge Pattern (Writing)*

In binary digital storage, we deposit either zero charge or a finite amount of charge at a large number of storage sites on the target. The useful area of a storage zone at each site is determined by the size of the beam. This is large enough to include, on the average, six small grid orifices. There is no attempt to register the beam with the fine structure of the barrier-grid and the beam may be allowed to fall on any portion of the target. In digital use, the deflection voltages must be rather precisely quantized so that the beam will strike repeatedly only at regularly spaced storage sites. The various sites may be designated or numbered in any desired way. Such a number or designation of a particular site is an "address" at which a digit may be stored.[3]

The mechanism of charge accumulation requires that the mica surface have a secondary emission ratio greater than unity, so that on the average each electron from the beam will release more than one secondary from the surface. If these secondaries are allowed to escape there will be a net loss of electrons from the surface which results in the accumulation of positive charge. If, on the other hand, these secondaries are returned to the surface, negative charge accumulates. When the potential of the mica surface is more negative than the grid, the secondaries escape and the potential of the mica surface rises. Conversely, when the mica has a potential substantially positive with respect to the grid, the second-

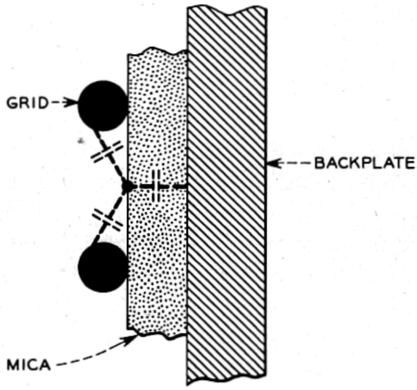

Fig. 3 — Capacitance distribution between the barrier grid, the dielectric surface, and the backplate.

[3] In most of our experiments the zones were spaced in a square lattice to obtain 16,384 sites in an area 1⅜ inches on each side. This number is 2^{14} which allows us to designate the sites with a 14 digit binary number. Seven of these digits may be used to specify the vertical deflection voltage and seven the horizontal.

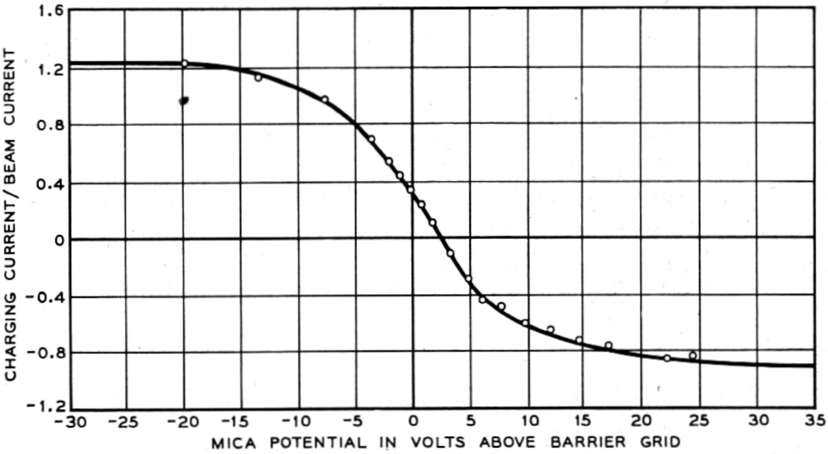

Fig. 4 — Charging curve at the mica surface showing the ratio of the charging current to the beam current as a function of the estimated potential difference between the dielectric surface and the barrier grid.

aries are returned and the potential drops. In each case the potential approaches an equilibrium value slightly more positive than the grid. At this potential the number of secondaries which escape is just equal to the number of primaries which arrive.

A degree of control over the potential of the mica surface may be obtained by varying the potential of the backplate behind the mica. One may visualize an equivalent circuit at the mica as indicated in Fig. 3. Here we picture capacitance distributed between the barrier-grid, the dielectric surface, and the backplate. Measurements indicate that on the average, 60 per cent of the backplate voltage change appears at the face of the mica with the barrier-grid at ground potential.

Fig. 4 shows the charging current as a function of the mica potential. This curve has a rounded characteristic partly because of the velocity distribution of the emitted secondary electrons. It is even more broadly rounded because of such effects as charging and discharging under the grid wires, redistribution of secondary electrons from the grid, and geometrical factors producing non-uniform electric fields. The curve of Fig. 4 was obtained by an indirect method using a broad, defocused electron beam sweeping over a large area.

In storing binary information, the backplate potential is switched between two voltages, usually 50 volts apart. Suppose that the beam has previously bombarded a spot until the equilibrium potential has been reached at the mica surface, and that we then apply a positive step-function voltage at the backplate. The front face of the mica rises instantaneously to a new value and negative charge begins to accumulate under the action of the electron beam. This causes the potential at the mica surface to fall rapidly and approach the same equilibrium value that it had before step-function was applied. We might now wait until the equilibrium is re-established and then turn off the beam and return the backplate to its previous potential. This will cause a drop in the mica potential below the equilibrium value. When the beam is again turned on, positive charge will accumulate, driving the potential up again toward the equilibrium value. During the time that negative charge is accumulating, the number of secondary electrons which escape from the target is less than the number when the mica has reached equilibrium. Conversely, when positive charge is accumulating, there is a temporary excess in secondary electron current over the equilibrium value. The output signal is obtained by detecting the secondary current. This output differs from the equilibrium value only during intervals of positive or negative charging of the mica. Such charging effects occur under the action of the beam during a short interval following any change in the backplate potential.

In describing the charging phenomena above, we have assumed a stationary beam. In actual service, we may *write* information at many sites by bombarding them successively for fixed time intervals. At each storage site we choose which of the two allowed backplate potentials to apply. At a later time, when we wish to *read* the information, we bombard the same spots but hold the backplate potential fixed at one of the two values. The signal types which are generated will be described in the next subsection.

3. *Reading Methods*

The reading signal is obtained by detecting the secondary emission current from the target. This may be accomplished either by measuring the net target current or by measuring the secondary current alone at the collector. These methods are called *target reading* and *collector reading*, respectively. For digital applications the target reading method offers several advantages over collector reading but collector reading is more convenient for image storage applications, which are not considered in this paper.

For digital operation, the beam is biased to cut-off except while performing either write or read operations at specific storage sites. Output pulses are generated by the tube whenever the beam is turned on. Either of two distinct types of pulses may be obtained while reading and additional types of output signal pulses may be generated during writing.

It is the function of the reading circuit and its associated amplifier and pulse discriminator to identify the stored binary digits.

During writing we bombard a number of spots, determining at each spot which of the two backplate potentials to apply. During reading, we return the beam to these spots but leave the backplate potential fixed at a potential which might be either of the two values used for writing. For reasons to be explained later, we choose to read at the more negative of the two values. Quite arbitrarily we designate an operation with the backplate positive as writing the binary digit *one*. An operation with the backplate at its more negative value is either a *write zero* operation or a *reading* operation. There are four possible cases, considering the backplate potential both at the time of the operation and at time of the last previous operation. These are: (a) positive at present, positive previously (b) negative at present, positive previously; (c) negative at present, negative previously; and (d) positive at present, negative previously. These operations are designated by the following names:

(a) *write one* on *one*
(b) *read one* (or *write zero* on *one*)
(c) *read zero* (or *write zero* on *zero*)
(d) *write one* on *zero*

In usual digital applications, an output signal is needed only during the (b) and (c) operations. The data presented in later sections deal only with these two types but in this section we will describe qualitatively all four signal types, which some modes of operation may require.

From previous discussions, it is apparent that operation (a) should give only the equilibrium secondary current leaving the target, operation (b) should give an excess secondary current, (c) should produce the equilibrium secondary current and (d) should produce less than the equilibrium secondary current.

The character of the output signal pulses differ in the collector and target reading methods. In collector reading, the secondary electrons arrive at the collector and generate a negative voltage proportional to the current. In target reading we detect the net current to the target which is the difference between the beam current and the secondary current.

Fig. 5 shows the waveforms associated with the collector reading method for each of the four possible cases. The top curve indicates that the beam is turned on for a short time to perform each operation, and is off between operations. In the same time sequence, we show the backplate potential switched to a positive value for *write one* and held at zero for reading. The third curve is an idealization of the collector current pro-

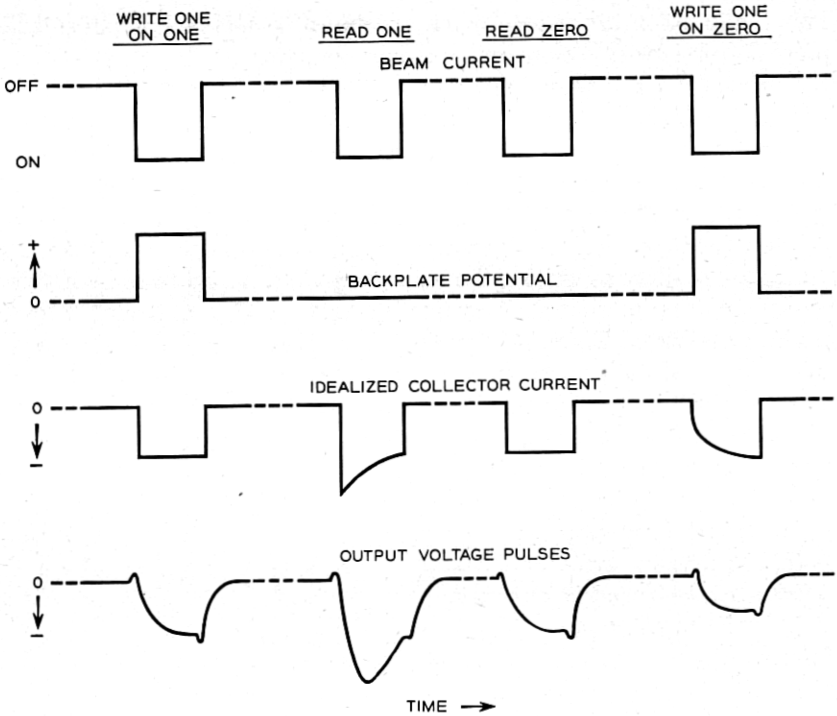

Fig. 5 — Signals obtained for four cases in binary signal storage, using collector reading.

duced in each operation. In cases (a) and (c) there is no change in the voltage condition of the surface and the current is constant at the equilibrium value. In the *read one* case, (b), the surface charges in the positive direction so that there is an excess current of secondary electrons to the collector. Because of rounded nature of the charging curve of Fig. 4, the excess current decreases as the surface charges toward equilibrium, producing the current pulse shown in Fig. 5. The pulse waveform depends on the amount of stored charge, the capacitance of the surface, and on the exact shape of the charging curve of the tube being investigated. In the case of *write one* on *zero*, (d), the surface charges in the negative direction so that less than the equilibrium current reaches the collector. The current gradually increases to the equilibrium value as the dielectric surface approaches the new equilibrium potential.

Experimental output voltage pulses found in our investigations are shown in the bottom curve of Fig. 5. The signal voltage is produced across a load resistor between the collector and ground. The rise and fall times are determined primarily by the product of the collector capacitance and the load resistance. A *read one* output signal has the same polarity as a *read zero* signal, so that differentiation between the two types of output signals requires amplitude discrimination.

In collector reading, we detect only the electron current reaching the collector from the target structure. Some of the current from the target goes to the shield and is not utilized. Since the division of current between the shield and the collector depends on the position of the spot bombarded by the beam, a method which detects the total current leaving the target is desirable. This current can be detected by measuring the sum of the currents leaving all of the electrodes in the target structure. During the *write one* operation, however, a pulse of the order of 50 volts is applied to the backplate. Since the output signal is of the order of one millivolt, the reading circuit must be isolated as completely as possible from the writing circuit in order to prevent overloading the sensitive reading amplifier.

A target reading circuit which accomplishes this isolation is illustrated in Fig. 6. The basic circuit is a coaxial line which is coiled to form an inductance. The outer conductor is grounded at one end and is enlarged at the other end to surround the end of the tube and connect at

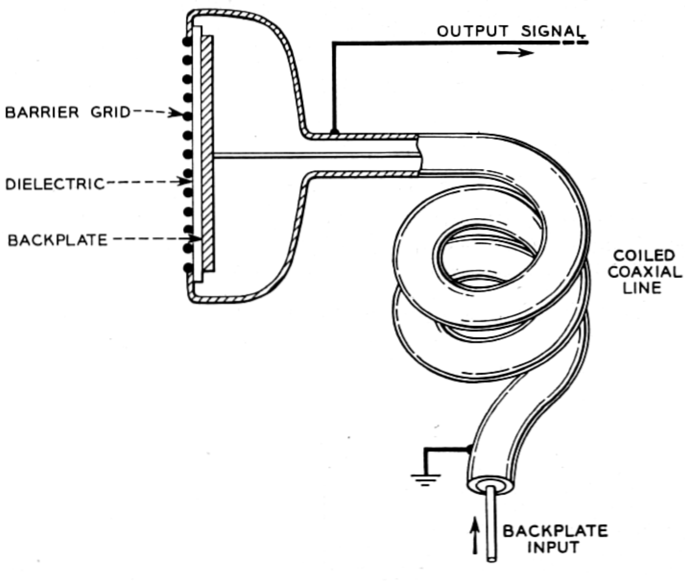

Fig. 6 — Schematic sketch of the circuit used for target reading in the barrier-grid storage tube. In these experiments, the coaxial line was wound on a ferrite core to obtain an adequately high inductance.

several places to the periphery of the barrier-grid. At the tube end, the outer conductor, which now includes the barrier-grid, completely encloses the backplate and shields it from ground. Upon application of a backplate pulse, current flows along the inner conductor to charge the barrier-grid to backplate capacitance, and ideally, all of this current should return through the outer conductor. Under these conditions no signal voltage should appear between the barrier-grid and ground because these currents should cancel each other and cause no voltage drop across the inductance. A net electronic current to the target, however, may divide between the inner and outer conductors in a parallel sense and thereby generate a signal whenever a change in this net current occurs. Ordinarily, the circuit is heavily damped with a shunt resistance from barrier-grid to ground to prevent ringing effects following signal generation.

Under equilibrium conditions, the effective secondary emission ratio of the target (including the grid and mica) is slightly less than one. Consequently, the *read zero* signal in this case is a small net negative current to the target within the tube. During intervals of charge accumulation on the mica, the net current will differ from this value. While accumulating positive charge (*read one*), the net current is somewhat positive and while accumulating negative charge (*write one* on *zero*) the current is more negative than the *read zero* signal.

Fig. 7 shows the waveforms associated with the target reading method. The beam current and backplate are switched for the various sequences as indicated at the top of the figure. The total secondary current which leaves the target is shown in the third curve. The net target current is the sum of the secondary current and the beam current. We also show output signals drawn from typical waveforms found in our investigations. The target reading circuit does not respond to the dc and low frequency components in the current pulses. The output pulses have an appearance similar to heavily damped sine waves. In the sketches in Fig. 7, the resonant frequency of the inductance and the stray capacitance between the barrier-grid structure and ground has a period roughly equal to the time the beam remains on. The output signals were measured with critical damping. The pulse shapes agree with those calculated from the circuit constants. The output of the reading amplifier should pass through a sampling gate which allows transmission only during a short time interval. The final gated response is shown on the bottom line of Fig. 7. The *read one* output signal is seen to have a polarity opposite to that of the *read zero* signal.

There are several advantages to the target reading scheme for binary digital storage. First, since the *zero* and *one* responses are of opposite

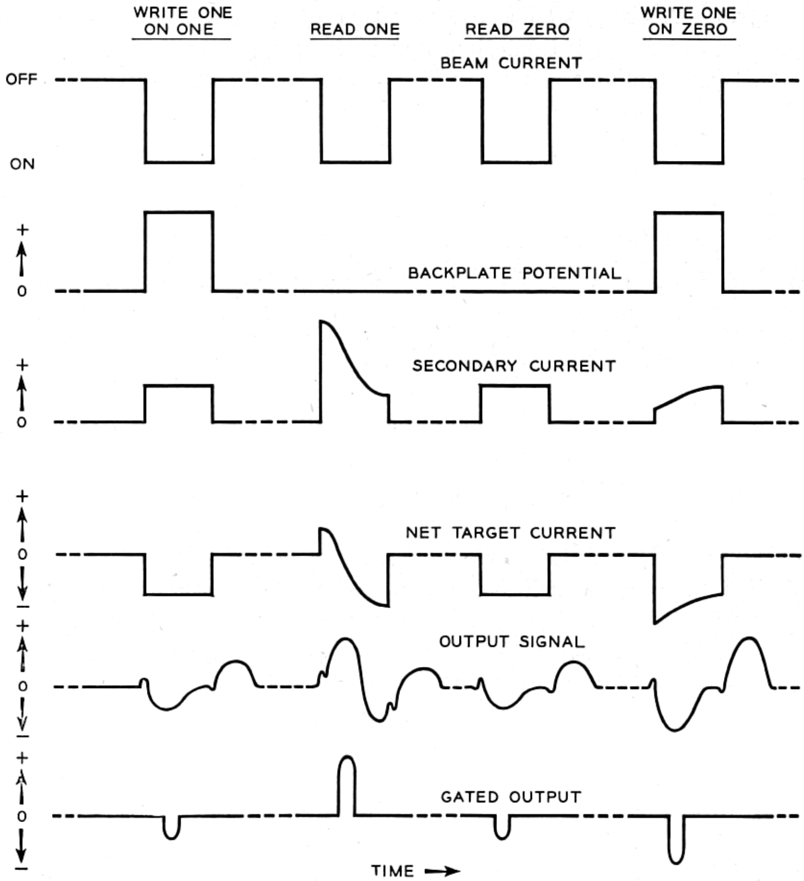

Fig. 7 — Currents and signals generated with the target-reading circuit of Fig. 6 for the four cases of Fig. 5.

polarity, the threshold decision level is near zero. This makes the output less sensitive to changes in beam current, which otherwise would require changes in the threshold level. Another advantage is that all of the secondary electron current from the target assembly is used for signal generation and there is no problem, as in collector reading, of obtaining uniform collection of secondaries from the various areas of the target surface.

4. *Regeneration*

In some conditions of operation, it is desirable to retain information in the tube after it is read. It is possible, by the use of external circuitry, to rewrite any binary digit before moving on to the next spot. This operation is called regeneration. Regeneration is required periodically at all spots if information is to be retained for long periods. Otherwise, the pattern will deteriorate because of resistive leakage in the dielectric and because of neutralization by positive ions and scattered electrons. Similarly, if a random-access program is used, slight overlapping of the storage elements may result in erasure or false writing at one site if repeated operations are performed at adjacent sites. These effects can be minimized by periodic regeneration of all stored information.

III. SIGNAL VARIATIONS

1. *General*

With an ideal binary storage device one would expect to obtain only two types of output reading signal, depending upon whether a *zero* or a *one* is being read. These two types should be clearly distinguishable from each other, either by the magnitude or character of the signals. Furthermore, within their separate groups, all *one* type signals and all *zero* type signals should be identical. In a practical device working at its maximum capacity, the signals will not be ideal in this sense and appreciable variations will be observed within the *zero* and *one* type signal groups. It is a characteristic of binary systems that such variations can be tolerated provided that they are not sufficiently great that there is danger of interpreting a *zero* as a *one* or interpreting a *one* as a *zero*. In the remainder of this section we will describe the various types of signal variation and their causes.

2. *Shading*

Shading is a gradual variation in output signal over the surface of the storage target. Usually the signals are strongest at the center and weakest at the edge. One cause of shading is the finite angle of primary beam incidence for storage sites near the edges of the target. Appreciable charge accumulates under the grid wires where the escape of secondary electrons is somewhat inhibited. This effect appears both in target and collector reading schemes. When collector reading is used, there is additional shading because the fractional collection of secondary electrons is not uniform over the target surface, causing variations in the *zero* response as well as the *one* response.

A third cause of shading arises from defocusing of the electron beam by electrostatic deflection. This is a serious problem where wide angles of deflection are used. It is an inherent defect in electrostatic deflection and cannot be eliminated by any degree of careful tube design. Pierce[4] shows that a set of deflection plates acts as a cylindrical converging lens whose focal length f is given approximately by the formula

$$\frac{1}{f} = \frac{2\theta^2}{l},$$

where θ is the angle of deflection and l is the length of the plates in the direction of the beam axis. Since the angle of deflection is directly proportional to the deflection voltage the focusing effect varies with the square of the deflection voltage. A correction voltage can be fed back from the deflection plates to the Einzel lens to compensate for this additional focusing. Experiments have been performed which verified that the required correction is proportional to the square of the deflection voltage. In the tubes used for these experiments, the maximum storage capacity can in fact be obtained only by the use of dynamic correction methods which compensate for this change in the focusing characteristics.

The shading variation across the target surface for both collector and target reading methods are shown in Fig. 8. Here we show the *zero* and *one* outputs along a line through the target center. The line is at a 45° angle to the deflection axes. In obtaining the data for these curves, a deflection defocusing correction was made. There is less shading with target reading than there is with the collector reading method.

3. *Texture*

Small variations in signal occur because the barrier grid is not sufficiently fine in mesh compared with the size of the beam. A slightly different signal is produced when the beam is centered over a grid hole than when it is centered at an intersection of grid wires. The beam thus resolves the mesh to some extent. Spotty variations also occur in the secondary emission characteristic of the barrier grid. The maximum variation in output pulse height from both of these effects is ±10 per cent.

4. *Blemishes*

Occasional variations in the storage and secondary emission characteristics are noted at spots on the mica surface. These may be caused by imperfections in the natural mica or by contamination with foreign matter. With care in selection of the mica and with additional care in tube

[4] J. R. Pierce, Theory and Design of Electron Beams, D. Van Nostrand and Co., 2nd Ed. 1954, pp. 41–46.

cleaning and assembly, blemishes are rarely observed which are of sufficient importance to cause errors in memory.

5. *Incomplete Erasure*

Whenever the potential at a spot is changed, the charging proceeds rapidly at first and then approaches the equilibrium condition in a manner similar to an exponential decay. In practice, one cannot wait an indefinite time to reestablish the equilibrium at each operation. This is further complicated by the non-uniform current density in the beam which does not allow the edges of the zones to become charged to equilibrium in normal operation. If the time of operation is prolonged, charge can continue to accumulate at the edges long after the center becomes saturated.

We shall now analyze an over-simplified model in order to obtain a

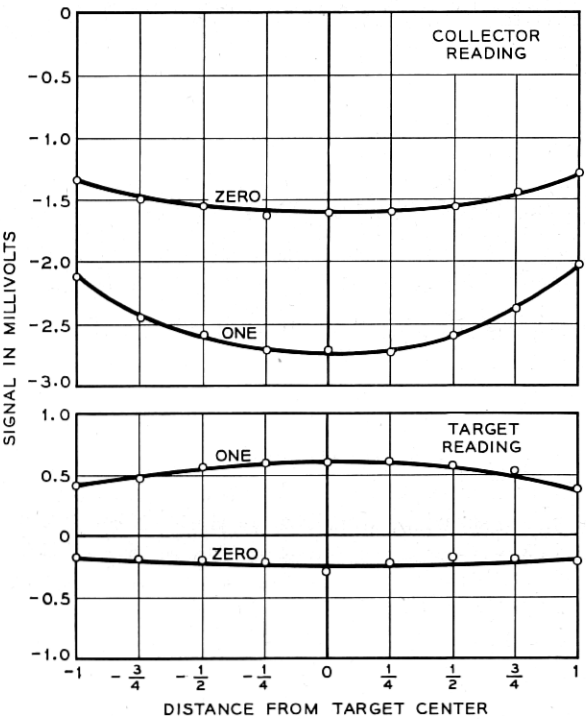

Fig. 8 — Shading characteristics for one microsecond reading and writing times. Data were taken along a diagonal through the center of the useful square area.

qualitative understanding of this behavior. We assume that the charging rate is proportional to the current density alone and that its magnitude is independent of the voltage difference between the grid and mica. The charging rate is positive for mica voltages below equilibrium and negative for voltages above. This is equivalent to assuming that the charging curve of Fig. 4 is a step-function, positive to the left of zero and negative to the right. We further assume that the beam has an ideal Gaussian variation of current density with radius (r) given by

$$J(r) = \frac{I_b}{2\pi\sigma^2} e^{-(r^2/2\sigma^2)} \tag{1}$$

where $J(r)$ is the current density, I_b is the beam current and σ is the measure of beam width.

As an initial condition, we assume that the surface has been brought to equilibrium with the backplate in its more negative state. We then raise the backplate to its positive state and perform a *write-one* operation at a fixed spot for an indefinite time. We wish to determine the character of the surface charge distribution which accumulates as a function of time. We also wish to know how this charge is removed in a subsequent reading operation. At each infinitesimal portion of the area, the charge accumulates in proportion to the local current density up to the saturation value. At first we obtain a simple Gaussian distribution growing linearly with time. After an interval which we designate as t_0, the center of the spot becomes saturated and the zone of saturation grows over an ever increasing area.

Fig. 9 illustrates the effect we are describing in this section. This figure shows several curves of charge density vs radius for various writing and

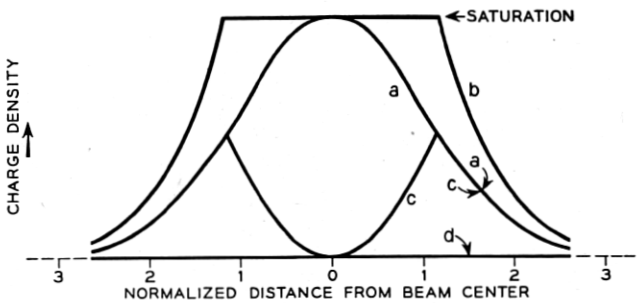

Fig. 9 — Charge density versus radius at a spot at various stages when the writing time and reading time are each 2 t_0. At curve (a) we have written for t_0 and at curve (b) we have finished writing at 2 t_0. At curve (c) we have read for an interval t_0 and at (d) we have finished reading after 2 t_0.

longer time for reading than for writing in order to obtain sufficiently complete erasure.

The previous analysis is greatly oversimplified but qualitatively explains the necessity of a program which allows sufficiently long reading times to remove previously deposited charge. In actual practice, the rounded character of the charging curve of Fig. 4 modifies this picture considerably, especially in those regions at the edge of the beam where the charging action is weak. This may cause a very slow drift in the potential of the dielectric surface in this region, depending upon the relative frequency of reading and writing operations over an appreciable period of time. Thus the extent of charging in the areas between spots in a spacial array will depend upon the particular storage program.

The output signals on reading are affected to some extent by the presence of charge in the intermediate regions, so that we can expect a certain amount of variability in the output depending upon the recent history of *write zero* and *write one* operations. One observed consequence is that we obtain larger signals from stored *ones* as the frequency of *write one* operations increases in comparison with *write zero* operations.

If we alternately *write one* and *read* at a particular site over a long period of time, the read output signal may be as much as 40 per cent larger than that obtained when the frequency of *write one* operations is very low. Thus, we find a significant source of signal variation caused by incomplete erasure. These effects may be minimized by restricting the program so that a reading operation precedes each *write one* operation or by allowing an adequately long reading time compared to the writing time.

6. *Overlap*

Another consequence of the Gaussian distribution of current density is that there will be a slight overlap of the storage elements, as defined by the beam. If two spots overlap slightly, repeated reading at one spot will tend to erase slowly a *one* signal stored at the other. Similarly, repeated writing of *ones* at a given spot will gradually cause a *one* to appear at an adjacent spot which is initially at *zero*. A measure of the seriousness of this effect is the "read-around-ratio," which is defined as the number of times that reading, writing, erasing, or regenerating operations may be performed at one spot without destroying information at an adjacent spot. Read-around-ratio and resolution (i.e., the number of storage sites per unit area) are interdependent, so that less interaction between spots can be obtained by reducing the number of storage sites. Conversely, an increase in the number of storage sites reduces the read-around-ratio. The relationship between read-around-ratio and distance between storage sites was found experimentally in a typical tube and is shown in Fig. 11. An amplitude degradation of 25 per cent of maximum was used in the measurements for the read-around criterion. The solid curve represents the relationship which would be expected on a simple theory based on the Gaussian distribution of current density. This curve is drawn for a σ of 0.0026″ which agrees well with independent measurements of spot size. The difference between the theoretical values and the data for larger distances between storage sites may be due to redistribution of secondary electrons, to scattering of electrons from the edges of the gun apertures and to electron optical effects such as lens aberrations and space charge.

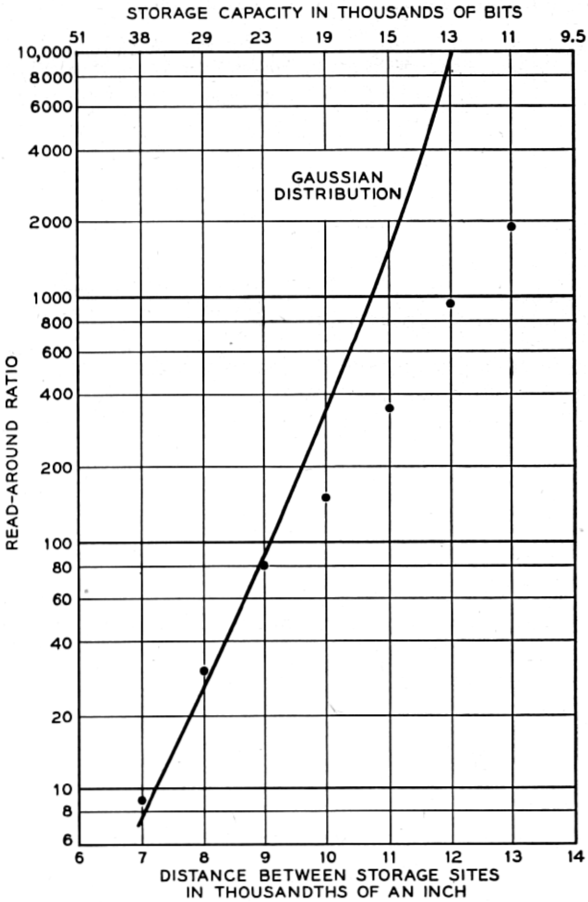

Fig. 11 — Read-around ratio and storage capacity as a function of the distance between adjacent storage sites.

7. *Noise*

Any perturbing noise phenomenon will affect the uniformity of the output signal. The beam current contains the usual fluctuation noise arising from the random times of emission of electrons at the cathode and from the velocity distribution of emission. To this must be added some additional noise because secondary electrons are emitted in groups. There are, however, about 10^7 electrons in each signal pulse and the probability of this number varying significantly because of shot effect is entirely negligible. The random noise generated in the reading amplifier can, however, be a significant source of error if the amplifier is poorly designed or if the signal strength is too weak. The effects of amplifier noise will be discussed later.

Man-made noise and interference pickup of various kinds can also be a significant source of apparent signal variations. For example, it has been found necessary to shield the deflection plates from the collector to reduce interference in collector reading. Inasmuch as the output signal is of the order of one millivolt, considerable care must be used to eliminate all sources of interference caused by improper shielding, circulating ground currents, etc.

IV. OUTPUT SIGNAL CONSIDERATIONS

In any large capacity storage device where the storage sites are distributed in space we must expect a certain amount of variation in the output signals from the various sites. The diagram of Fig. 12 might represent the magnitudes of the two types of signals from each site in a binary store. Ideally, we would like these two groups of signal amplitudes to be well separated from each other in magnitude and to have the members of each group closely bunched together about their respective average values. In the barrier-grid tube it is possible to obtain such performance if one is overly conservative in the use of the tube by keeping the spots large and well separated and by using long operating periods. If the spots are more closely spaced, higher speeds are used, and random-access programs applied, the variations in signal become greater and the separation between the groups becomes less.

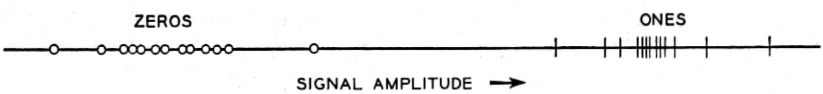

Fig. 12 — A possible set of signals from each site in a binary store, showing a range of signal variations.

It has been found convenient to express the signal characteristics and uniformity by means of a signal separation chart as shown in Fig. 13. On this chart, the output signal voltage is the abscissa and the ordinate represents numbers of storage sites. A square-root scale is used for the ordinate to emphasize the region of minimum signal separation. We plot two curves of the "integral" type. The curve on the left represents the total number of spots which give a *zero* response voltage greater than the abscissa; the curve on the right is the number giving a one response less than the abscissa. Each of these curves is measured using the program of operation most likely to produce an error. For example, the program of operation most likely to produce an error for a written *one* is as follows: Store *ones* at alternate spots in the array, read the remaining spots some

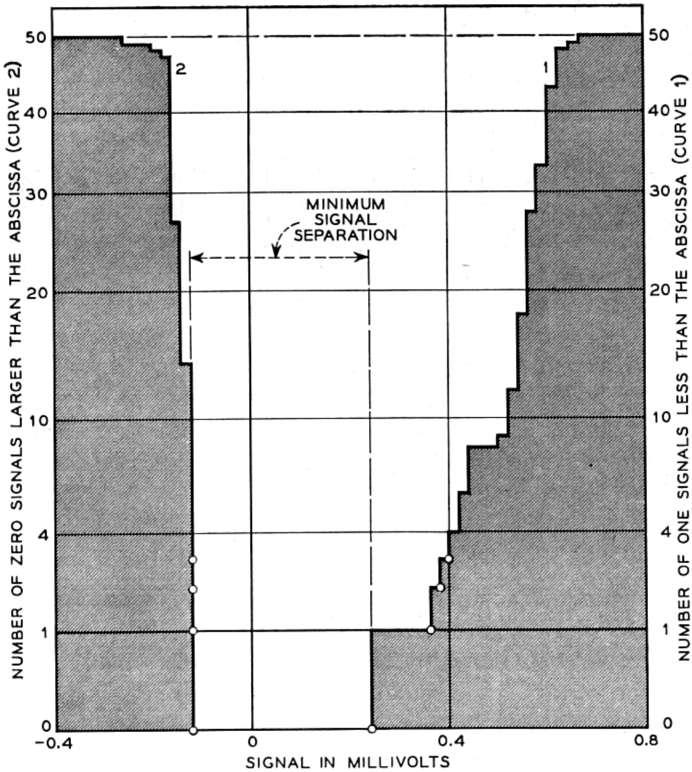

Fig. 13 — Signal separation chart for 50 scattered spots on the barrier grid storage tube. Curve 1 shows the "one" signals obtained after 100 reading operations are performed adjacent to the written spots. Curve 2 shows the "zero" signals obtained after 100 write one read sequences are applied to adjacent spots.

large number of times, then return and read the original group. We then record the amplitudes of the final reading signals and plot the results on the right side of the signal separation chart. The corresponding pessimistic program for the *zero* group is to *write zero* on alternate spots, then write alternate *zeros* and *ones* on the remaining spots for a large number of cycles, then return and read the original group. Plotting the distribution of the *zero* type outputs obtained completes the picture on the signal separation chart. The minimum separation between these curves gives an indication of the likelihood of error in a random-access type of service.

The signal separation chart is a representation of the total effect of the signal variations discussed in Section III. The effects of amplifier noise, however, are greatly reduced by our method of performing the tests, since the signal obtained for each spot is the average of a large number of repeated operations. The other signal variations either are systematic (shading, incomplete erasure and overlap) or have definite limits (texture). The storage sites used to obtain the data presented in Fig. 13 were chosen in such a way that the worst conditions contributing to systematic signal variations were included. Thus, the signal separation which was found between the maximum *zero* signal and the minimum *one* signal should be very nearly the same for a much larger number of storage sites. The minimum signal separation was found to be 0.36 millivolts out of a total signal spread of 0.90 millivolts. The data were taken using the target-reading method.

We will next determine the probability of error caused by amplifier noise. For this we assume that the input resistor is R ohms, the bandwidth is B cycles per second and that the noise factor[5] of the amplifier is F. Further we must assume that only random or Gaussian noise is present. The apparent rms noise voltage, V_n, at the input to the amplifier is given by[5]

$$V_n = \sqrt{4FRkT_0B}\,, \tag{6}$$

where T_0 is the standard noise temperature, 290°K, and k is Boltzmann's constant, 1.38×10^{-23} joules per degree.

A basic property of Gaussian fluctuations is that the probability at any instant of the voltage lying between V and $V + dV$ is given by[6]

$$P = \frac{1}{V_n\sqrt{2\pi}}\, e^{-(V^2/2V_n^2)}\, dV\,. \tag{7}$$

---

[5] Stanford Goldman, Frequency Analysis, Modulation and Noise, McGraw-Hill, 1948.
[6] Ibid, p. 206.

Integrating from V to infinity gives the probability, $P_{>V}$, that the noise voltage will be greater than V. This gives

$$P_{>V} = \frac{1}{2}\left(1 - \frac{2}{\sqrt{\pi}} \int_0^{V/\sqrt{2}V_n} e^{-x^2}\, dx\right) \tag{8}$$

The second term inside the parenthesis is the familiar error integral given in Pierce's integral tables.[7] Suppose, now, that V represents the voltage difference between a given signal and discrimination level (threshold). The probability of error, due to noise, for *that* signal is given by equation (8), substituting for V from equation (6).

It is interesting to assume some reasonable numbers for the amplifier characteristics and determine the minimum allowed signal voltage V to obtain an arbitrarily chosen probability of error. We assume a program such that 10^6 operations are performed per second. Thus a probability of error of 4×10^{-13} corresponds to one mistake per month of continuous operation. We also choose an amplifier with a bandwidth of two megacycles per second and a noise factor of 2. A typical input resistor has a value of 2,000 ohms. Under these conditions we calculate from (8) that a minimum signal of 80 microvolts measured from threshold is allowed. A separation of 360 microvolts was found on the signal separation chart. There is, therefore, a negligible probability of error due to amplifier noise alone. Variations in the voltages applied to the storage tube or drift in the output circuit can combine with noise to produce errors unless care is taken to provide stable external circuitry.

V. SUMMARY

The barrier-grid storage tube as a binary digital memory device requires special conditions of operation. The margin of safety with regard to the likelihood of error depends upon the speed of operation, the type of program applied, and the spacing of storage sites on the target. The probability of error depends upon the minimum separation of *zero* and *one* type output signal amplitudes and upon the noise factor of the output amplifier. This probability may be made vanishingly small if the method of operation is conservatively chosen. Careful investigation of all these factors indicates that with a laboratory model of a storage tube, reliable operation is possible with 16,000 bits of stored information per

[7] B. O. Pierce, A Short Table of Integrals, Gin and Co., pp. 116–120, 1929, For large values of the argument we can use the semiconvergent series.

$$\frac{2}{\sqrt{\pi}} \int_0^{y} e^{-x^2}\, dx = 1 - \frac{e^{-y^2}}{y\sqrt{\pi}}\left(1 - \frac{1}{2y^2} + \frac{3}{(2y^2)^2} - \cdots\right)$$

tube, a read-around-ratio greater than 100, and a characteristic time of about one microsecond per operation.

IV. ACKNOWLEDGMENT

R. W. Sears was directly responsible for the earlier exploratory development phases of barrier-grid storage tubes in our laboratories and his continued guidance has been invaluable. H. C. Jonas carried out the mechanical phases of this work.